Materials Research. 2018; 21(5): e20171082
DOI: http://dx.doi.org/10.1590/1980-5373-MR-2017-1082

Silicon Nanostructuring Using SF_6/O_2 Downstram Plasma Etching: Morphological, Optical and Sensing Properties

Saker Saloum[a]*, Mohammad Ali Zrir[a], Bachar Alkhaled[a], Samer Abo Shaker[a]

[a]*Physics Department, Atomic Energy Commission of Syria (AECS), P.O. Box 6091 Damascus, Syria*

Received: December 11, 2017; Revised: April 23, 2018; Accepted: June 05, 2018

Silicon (Si) nanostructures were prepared in the downstream of radiofrequency SF_6/O_2 mixture plasma generated in 13.56 MHz hollow cathode discharge system. Depending on the oxygen percentage in the mixture, the obtained Si nanostructures were characterized for their different properties: etching rate, morphology, optical reflectance, photoluminescence, spectral response and humidity sensing. It is found that the etching rate exhibits a maximum value when the O_2 ratio reaches 5%. An interesting defect-induced "violet" luminescence is reported from the Si nanostructures, whose intensity depends on their density. The obtained Si nanostructures have shown to induce a spectral response (SR) enhancement, in comparison with a smooth Si substrate, of about 100 times at 1100 nm wavelength. A very short response time (1 sec) to the humidity was measured for 5% O_2 in the SF_6/O_2 plasma mixture, which was found to be well-correlated with the porosity of the Si nanostructures.

Keywords: *Silicon nanostructures, SF_6/O_2 plasma etching, AFM, photoluminescence, spectral response, humidity sensing.*

1. Introduction

Silicon (Si) nanostructures have a broad, emerging application spectrum ranging from optics and optoelectronics over chemical and biological sensing to photovoltaics.[1-3] The so-called 'Black Silicon' (b-Si) describes nano or micro textured silicon surfaces,[4] it can be produced by Si surface etching using plasma technique, which is compatible with the silicon fabrication technology.[4-8] Plasma is a versatile and environmentally friendly technique which uses gases as reactants to modify materials surface. Gas discharges environments have active species such as ions, free radicals, electrons, molecular fragments and photons that are simultaneously generated and can induce surface modification of different materials. Etching is well-known as a consequence of plasma surface activation that results in morphological changes. SF_6/O_2 plasma mixture, providing the highly reactive etchant fluorine atoms, is widely used for silicon surface nanostructuring,[9-14] where the resulted Si nanostructures exhibited remarkable enhanced anti-reflective surface and light trapping efficiency, which is of great importance for photovoltaic applications to enhance the light absorption in Si solar cells.[10,11,13]

The technological motivation behind our present work is to investigate, besides the light anti-reflection property, other potential applications of the Si nanostructures using the maskless SF_6/O_2 plasma etching, such as light emitting (photoluminescence), photo-sensing (spectral response) and humidity sensing. In addition, this contribution will focus on the possibility of tuning these properties through varying the percentage of oxygen in SF_6/O_2 plasma mixture, and on the relationship of different obtained properties to the etching rate, the surface morphology and the SiO_xF_y self-masking layer formation. SF_6/O_2 plasma mixture will be generated in a low-pressure 13.56 MHz hollow cathode discharge (Plasma Consult GmbH PlasCon HCD-L300 System), which generates an intense (high density) primary plasma and a very homogeneous remote plasma.[7]

*e-mail: pscientific2@aec.org.sy.

2. Experimental Procedure

The experimental set-up of the HCD-L-300 system is described elsewhere.[7] A grounded stainless-steel substrate holder (70 x 70 x 1 cm^3) was located downstream at a distance of 45 mm below the plasma source. Four silicon wafers *n*-type Si (<100>, ρ ~1-20 Ω.cm, thickness ~ 500 μm) were etched in SF_6/O_2 plasma mixture during 30 min under experimental conditions described in Table 1. The applied RF power and the total pressure are fixed at 300 W and 50 Pa, respectively. The SF_6 gas flow rate is fixed at 200 sccm, while the flow rate of O_2 gas was varied as follows: 0 sccm, 10 sccm, 20 sccm and 30 sccm; thus the samples will be given the names SO-0, SO-10, SO-20 and SO-30 accordingly. The etch rate

Table 1. Experimental conditions for silicon wafers etching in SF6/O2 plasma: Applied RF power = 300 W, chamber pressure = 50 Pa, and etching time = 30 min

Sample	SF_6 flow rate (sccm)	O_2 flow rate (sccm)	O_2 percentage (%)
SO-0	200	0	0
SO-10	200	10	~ 5
SO-20	200	20	~ 9
SO-30	200	30	~ 13

was determined from the measurement of the etching depth determined from the weight loss of the silicon wafer after etching using a microbalance. The surface morphology of the etched Si was studied using Atomic Force Microscope (AFM - Park Scientific Instruments AP-0100). A Jobin-Yvon, Triax 550, UV/VIS/NIR computerized spectrophotometer is used to measure the optical reflection of the plasma etched silicon wafers, in the condition of near normal incidence (angle of incidence ≅ 1.5º) and within the spectral range 400-1200 nm with a step of 1 nm. The spectral response (SR (A/W) = short current density/incident light power flux) of the bulk Si and the obtained Si nanostructured is measured using a Tungsten-Halogen lamp as a light source, a spectrophotometer (Triax 550), and an automated data acquisition Keithley 237 electrometer in the spectral range of 400-1200 nm. The PL spectra were recorded at room temperature (RT) using a 1 m monochromator (SPEX) equipped with a side-on photomultiplier tube R928, where a He-Cd laser (wavelength of 325 nm) was used as an excitation source. The humidity sensing property of the nanostructured surfaces was performed by exposing the samples to a humid air (RH% = 80%) and recording the dynamical electrical response to obtain the response time of the sensor, while a constant voltage of 10 V is applied to the samples.

3. Results and Discussion

3.1 Etching rate

After measuring the etching depth, the etching rate of silicon in our SF_6/O_2 plasma is plotted as a function of O_2 percentage in the discharge in Figure 1. It can be seen that it reaches a maximum value (1450 nm/min) at 5% of O_2 in the mixture. To have an idea about the correlation of the etching rate behavior with the etchant atomic fluorine concentration, we performed measurements of both atomic fluorine [F] and atomic oxygen concentrations [O] in our SF_6/O_2 plasma discharge using the actinometry optical emission spectroscopy as described in details previously, in[7] for [F], and in[15] for [O]. The concentration curves, shown in Figure 2, exhibit a maximum for [F] at about 23% of O_2 in the discharge, and a monotonic increase of [O] with increasing of the oxygen percentage. Knizikevicius[16] performed a simulation of Si etching in SF_6/O_2 plasma and found that at 27% O_2, the concentration of F atoms approaches the maximum value. From the two figures 1 and 2, one can conclude that, in our case, the decrease of the etching rate beyond 5% O_2 is not related to the decrease of F radicals concentration in the plasma. It is more probably related to the formation of the SiO_xF_y passivation layer, whose thickness increases with the oxygen content in the discharge.[9] Indeed, it is demonstrated that F and O react with Si to form the self-masking layer SiO_xF_y on the surface, which acts as etching inhibitor at certain points on the surface.[4] This passivation layer is not very stable and dissociates by heating or under the ion bombardment of the plasma.[9,10] Since our system is a remote plasma configuration, where the concentrations of ions and electrons are relatively low and the concentration of free radicals is relatively high in the remote region far from the primary plasma,[17] the behavior of the etching rate as a function of O_2 content in the SF_6/O_2 plasma, may be related to the fact that the passivation layer resists the degradation by plasma ions bombardment in the downstream etching region. Thus, this layer plays a significant role in the etching rate lowering beyond 5% O_2 content. The competition between the formation of SiO_xF_y passivation layer and the Si etching by F atoms generally leads to the appearance of a maximum in Si etching rate as a function of O_2 content. The maximum value of the silicon etching rate depends on different operation parameters, such as the design of the plasma system, working pressure, applied power and O_2 content. In a Corial 200 IL operating at a frequency of 13.56 MHz (100 W), Wongwanitwattana et al.[12] obtained a maximum in Si etching rate (450 nm/min) for 5% O_2 in SF_6/O_2 mixture and a working pressure of 2.6 Pa. D'Agostino et al.[18] found a maximum in Si etching rate (about 400 nm/min) for 40% O_2 content in SF_6/O_2 capacitively coupled plasma

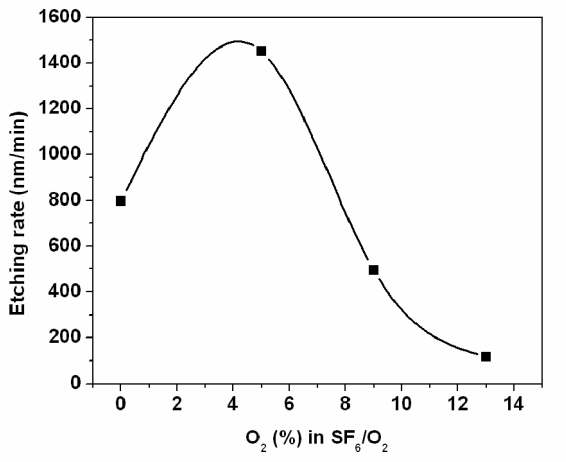

Figure 1. Variation of silicon etching rate in SF_6/O_2 plasma as a function of O_2 percentage

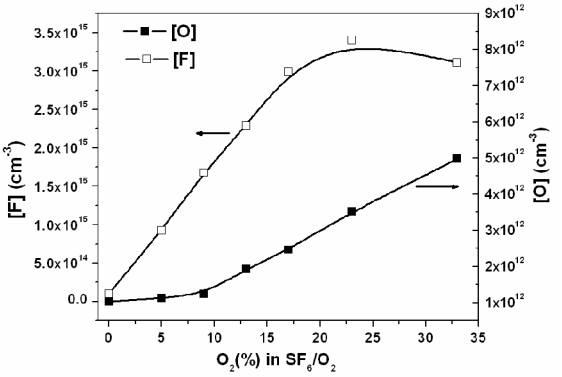

Figure 2. Variation of F atoms and O atoms concentration as a function of oxygen percentage in SF_6O_2 plasma

(CCP) driven by 27 MHz RF generator (45 W) at working pressure of 131 Pa. Zou[19] measured a maximum in Si etching rate (3000 nm/min) for 30% O_2 in SF_6/O_2 plasma and at a pressure of 26 Pa in an Oxford Instruments PlasmaLab 80+ reactive ion etcher with 13.56 MHz RF coupling (160 W).

3.2 AFM morphology

Figure 3 shows 2D AFM images (5 x 5 µm²) for the etched silicon surfaces: SO-0 (a), SO-10 (b), SO-20 (c), and SO-30 (d), together with their texture line profiles taken along the diagonal of the AFM image, which are traced for the same height scale [-500 , 500 nm]. These images reveal the formation of voids and roughened surfaces with different sizes of granules ranging from 80 nm to 1 µm. The variation of the total roughness (using *Gwyddion* software), the evolution of the mean pore and particle sizes (Diameter/Depth, Height), the porosity (the amount of voids within the Si nanostructured layer), and the particle density as a function of O_2 content in the SF_6/O_2 plasma are listed in Table 2. It can be noticed that, except of particle density, all these parameters has a maximum for the sample SO-10 (5% O_2), for which the etching rate has also a maximum. The correlation, in our case of RF remote plasma, between the etching rate and the roughness can be explained as following: For 5% of O_2 in the gas mixture, the SiO_xF_y layer is relatively thin and large denuded areas of the surface are expected. This results in a considerably higher etching rate and higher accompanied roughness induced by the etching of the large unpassivated areas (Fig. 3b). For higher O_2 content, the thickness of the passivation layer is increased.[9] Thicker passivation layers lead to more efficient inhibition of the etching, reducing the etching rate (Figure 1). This should also be accompanied with the reduction in the roughness, since it results from the etching process.

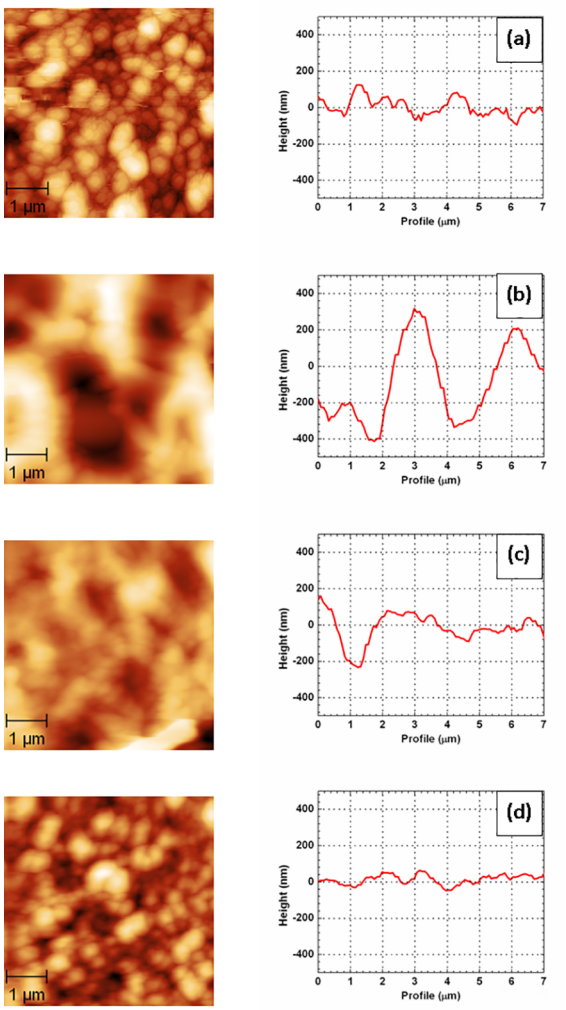

Figure 3. 2D AFM images (5 x 5 µm²), together with their texture diagonal profile, of SF_6/O_2 plasma-treated Si wafers as a function of O_2 percentage. (a): 0%, (b): 5%, (c): 9% and (d): 13%

3.3 Optical properties

3.3.1 Optical reflectance

Figure 4 displays the measured optical reflectance spectra of the etched Si samples (Table 1) in addition to a smooth Si substrate in the spectral range [400-1200 nm]. The inset shows the variation of average reflectance as function of O_2 percentage in the discharge. A significant decrease in the reflectance of the silicon surface after plasma etching can be observed, where the lowest reflectance (about 0.01%) was obtained for the sample SO-10. The evolution of optical reflectance as a function of O_2 percentage seems to be inversely proportional to the roughness of prepared samples, as can be illustrated in Figure 5 (average reflectance as a function of roughness). This means that the more surface is rough, the more light is being trapped in the Si nanostructure. This result was also demonstrated by other research groups.[10,11,13]

Table 2. AFM morphology parameters of the Si nanostructures formed by SF_6/O_2 plasma etching as a function of O_2 percentage.

Sample	Total roughness (nm)	Mean particle Diameter/Height (nm)	Mean pore Diameter/Depth (nm)	Porosity(%)	Particle density (μm^{-2})
SO-0	49	450/28	387/29	24	3.4
SO-10	195	830/105	940/141	39	0.6
SO-20	100	600/46	575/43	29	1.6
SO-30	33	503/21	475/23	19	2.6

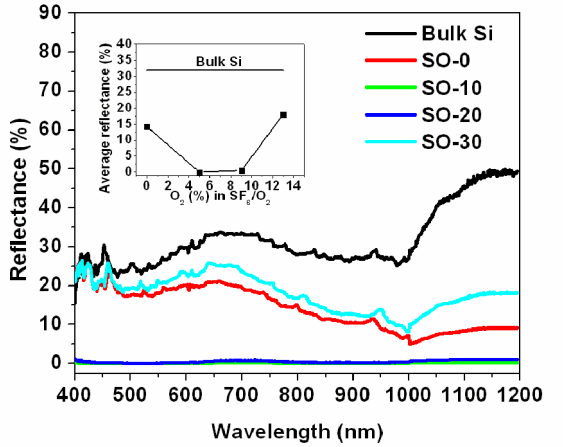

Figure 4. Optical reflectance spectra of etched Si samples (Table 1) and smooth silicon crystal. Inset: Variation of the average reflectance as a function of O_2 percentage in SF_6/O_2 plasma

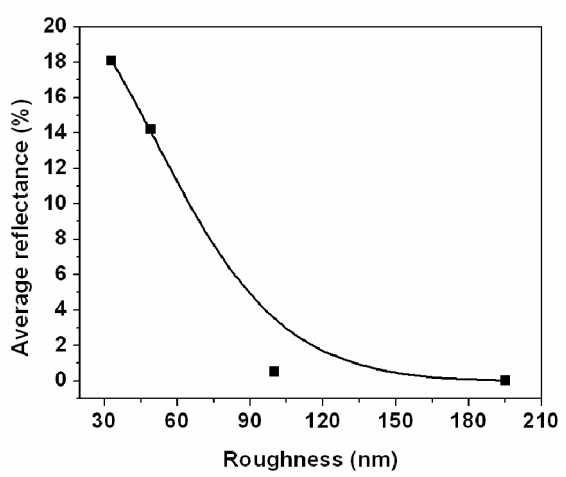

Figure 5. Plot of the average reflectance as a function of the surface roughness of different samples (Table 1)

3.3.2 Photoluminescence

Figure 6 exhibits the room temperature photoluminescence spectra of the etched Si samples listed in Table 1. The PL characteristic is "violet". The peaks positions are centered around 426 nm. It can be seen that there is no significant shift in the wavelength of the PL peak as a function of O_2 percentage in the SF_6/O_2 plasma mixture in spite of the significant difference in the particle size of the structures shown in Table 2. Therefore, the origin of this violet luminescence can't be attributed to quantum confinement effects.[20] It is more likely originated from luminescent defect centers.[21-23]Figure 7 shows the evolution of the integrated PL intensity as a function of the particle density of the Si nanostructures, the PL intensity has a minimum for the sample SO-10 (5 % O_2), which corresponds to the lowest particle density (Table 2), the maximum integrated intensity is observed for the sample SO-0 of the highest particle density. This behavior of PL intensity is probably due to the enhancement of the

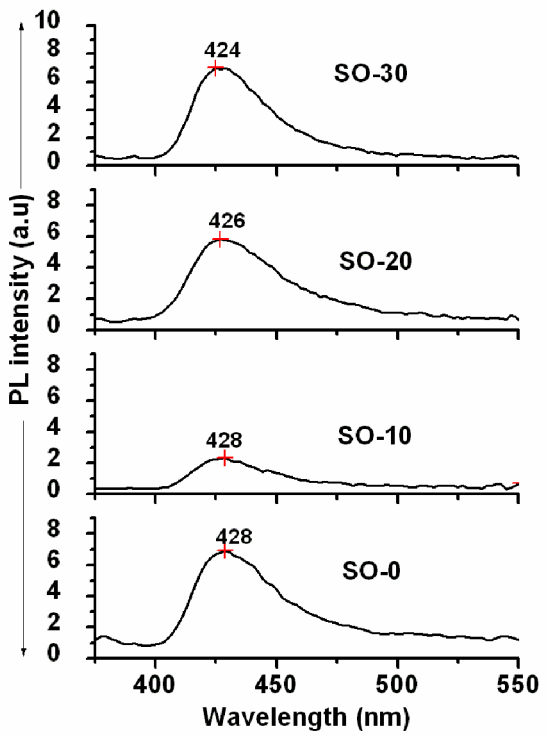

Figure 6. PL spectra of prepared samples (Table 1)

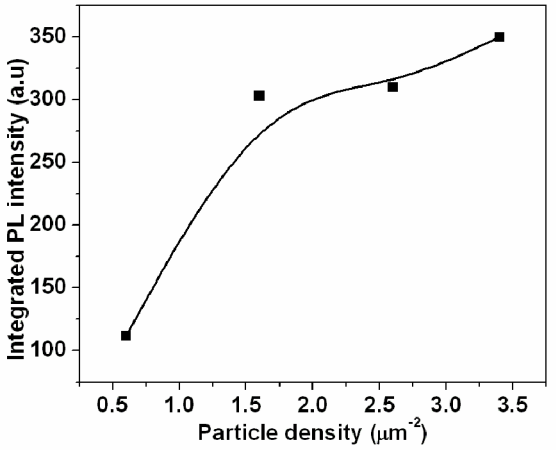

Figure 7. Variation of PL intensity of the fabricated Si nanostructures in the SF_6/O_2 plasma as a function of the particle density

light harvesting efficiency of prepared Si nanostructures with the increase of their particle density.

3.3.3 Spectral response

Figure 8 shows the evolution of the spectral response (SR) of a smooth Si substrate, SO-0, SO-10, SO-20 and SO-30 samples. A significant enhancement (about 100 times) of the SR, as compared to the reference sample (Bulk Si) after etching, can be observed around the band gap of Si (1100 nm ~ 1.12 eV). We attribute this significant enhancement of SR to the surface roughening of etched Si, which reduces

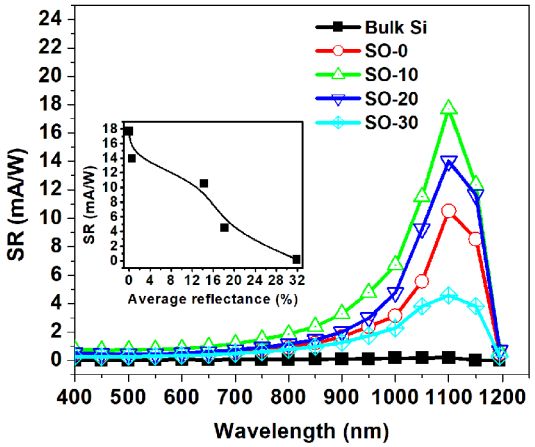

Figure 8. Spectral response (SR) spectra of etched Si samples (Table 1) and a bulk, smooth silicon wafer. The inset shows the plot of SR values at 1100 nm as a function of average reflectance

light reflection and thus improves light trapping.[11,13,14] At this wavelength, the SR changes depending on samples preparation conditions. It has a maximum at 5% O_2 (sample SO-10) that has the lowest reflectance (Figure 4). The inset of Figure 8 shows clearly an increase of SR with the decrease of average reflectance. These results are of great interest for photo-sensing applications and efficiency enhancement of silicon solar cells, where one can find some reported results about the enhancement of silicon solar cells performance after surface etching in SF_6/O_2 plasma. Yoo et al.[11] reported a correlation between c-Si solar cells parameters and the reflectance after etching in SF_6/O_2 plasma, where the cell efficiency was increased to be about 15.7%, for the ratio (SF_6/O_2=2), compared to 14.5% for the ratio (SF_6/O_2=3). Lin et al.[14] have successfully fabricated large-area (156 x 156 mm^2) anti-reflective (reflectance < 15%) surfaces of polycrystalline solar cells by self-masking RIE process using $SF_6/O_2/Cl_2$ plasma etching, where the solar cell efficiency was improved to be 16.27% comparing to the value of 15.56% when wet etching was used.

3.4 Humidity sensing property

By similarity to the Si nanostructures fabricated electrochemically,[24,25] the formation of pores in our nanostructures may result in good humidity sensing properties, which is of considerable importance in the field of silicon humidity sensors technology.

Figure 9 shows the dynamical electrical response to relative humidity (RH%=80%) of different prepared samples. The point (t= 0 sec) corresponds to the moment of sample exposure to the humidity, and the response time (t_r) corresponds to the moment at which the electrical resistance begins to be stable. As seen from the figure, the electrical resistance decreases when the samples are exposed to humidity, except

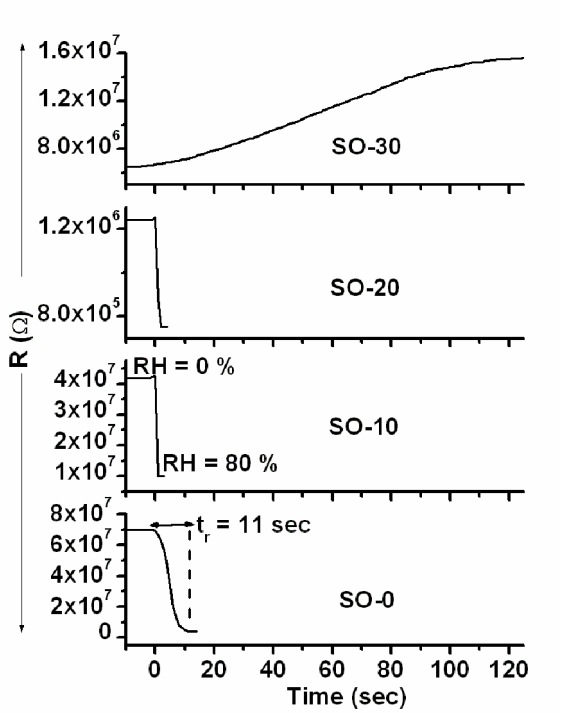

Figure 9. Dynamical electrical response to relative humidity (RH%=80%) of different prepared samples (Table 1)

of the sample SO-30. The sensitivity (S) was calculated using the following formula:

$$S = \frac{R_a}{R_h} \quad (1)$$

where R_h is the sensor resistance influenced by the humidity, and R_a is the sensor resistance in the ambient air. Table 3 summarizes the obtained response time and sensitivity of samples.

It can be seen that both t_r and S are influenced by the plasma preparation conditions of the Si nanostructures. Referring to AFM morphology data of Table 2, one can notice that the shortest response time (1 sec) corresponds to the highest porosity (sample SO-10). Figure 10 shows a clear correlation between the response time and the porosity. The long response time (120 sec) of the sample SO-30 (13% O_2) isn't only related to the lowest porosity, but also to a possible

Table 3. Response time and sensitivity of the Si nanostructures exposed to 80% humidity as a function of O2 percentage in SF6/O2 plasma.

Sample	Response time, t_r(sec)	Sensitivity, S (a.u)
SO-0	11	17
SO-10	1	4.3
SO-20	2	1.7
SO-30	120	0.4

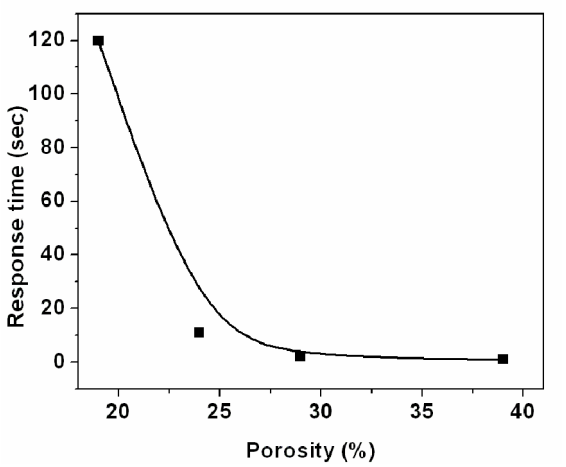

Figure 10. Plot of the response time to humidity of samples as a function of their porosity

passivation effect, where the passivation layer causes slow kinetics of absorption and diffusion for water molecules to pores, and this can explain also the abnormal behavior of the electrical resistance (Figure 9) of this sample SO-30. The sensitivity decreases as a function of O_2 percentage, from 17 (SO-0) to 0.4 (SO-30).

4. Conclusions

Silicon nanostructures have been successfully fabricated in downstream RF SF_6/O_2 plasma excited in a hollow cathode discharge system. The prepared structures have been characterized for their different properties (etching rate, morphology, optical reflectance, photoluminescence, spectral response and humidity sensing) as a function of O_2 percentage in the discharge. The highest etching rate, highest roughness and porosity, lowest reflectance, highest spectral response and shortest response time to humidity were found for the sample etched in the plasma mixture with 5 % O_2. The different properties of the Si nanostructures were found to be well correlated, where the evolution of the optical reflectance follows the surface roughness of the samples, the violet PL intensity increases with the particle density of the Si nanostructures, the spectral response is inversely proportional to the optical reflectance and the response time to the humidity depends on the porosity of the Si surface. The passivation layer SiO_xF_y seems to affect the etching rate, the PL intensity and the response time to humidity.

5. Acknowledgments

The authors would like to thank Prof. I Othman, Director General of AECS, for encouragement and permanent support.

6. References

1. Smith RL, Collins SD. Porous silicon formation mechanisms. *Journal of Applied Physics*. 1992;71(8):R1.

2. Westwater J, Gosain DP, Tomiya S, Usui S, Ruda H. Growth of silicon nanowires via gold/silane vapor-liquid-solid reaction. *Journal of Vacuum Science & Technology B*. 1997;15(3):554-557.

3. Her TH, Finlay RJ, Wu C, Mazur E. Femtosecond laser-induced formation of spikes on silicon. *Applied Physics A*. 2000;70(4):383-385.

4. Gaudig M, Hirsch J, Naumann V, Werner M, Großer S, Hagendorf C, et al. Elemental evolution of the SiOxFy self-masking layer of plasma textured silicon and its modification during air exposure. *Journal of Applied Physics*. 2017;121(6):063301.

5. Jansen H, De Boer M, Legtenberg R, Elwenspoek M. The black silicon method: a universal method for determining the parameter setting of a fluorine-based reactive ion etcher in deep silicon trench etching with profile control. *Journal of Micromechanics and Microengineering*. 1995;5(2):115-120.

6. Boulousis G, Constantoudis V, Kokkoris G, Gogolides E. Formation and metrology of dual scale nano-morphology on SF6 plasma etched silicon surfaces. *Nanotechnology*. 2008;19(25):255301.

7. Saloum S, Akel M, Alkhaled B. Diagnostic and processing in SF6 RF remote plasma for silicon etching. *Journal of Physics D: Applied Physics*. 2009;42(17):175206.

8. Kalem S, Werner P, Arthursson O, Talalaev V, Nilsson B, Hagberg M, et al. Black silicon with high density and high aspect ratio nanowhiskers. *Nanotechnology*. 2011;22(23):235307.

9. Dussart R, Mellhaoui X, Tillocher T, Lefaucheux P, Volatier M, Socquet-Clerc C, et al. Silicon columnar microstructures induced by an SF6/O2 plasma. *Journal of Physics D: Applied Physics*. 2005;38(18):3395-3402.

10. Steglich M, Käsebier T, Zilk M, Pertsch Th, Kley EB, Tünnermann A. The structural and optical properties of black silicon by inductively coupled plasma reactive ion etching. *Journal of Applied Physics*. 2014;116(17):173503.

11. Yoo J, Kim K, Thamilselvan M, Lakshminarayn N, Kim YK, Lee J, et al. RIE texturing optimization for thin c-Si solar cells in SF6/O2 plasma. *Journal of Physics D: Applied Physics*. 2008;41(12):125205.

12. Wongwanitwattana C, Shah VA, Myronov M, Parker EHC, Whall T, Leadley DR. Precision plasma etching of Si, Ge, and Ge:P by SF6 with added O2. *Journal of Vacuum Science & Technology A*. 2014;32(3):031302.

13. Moreno M, Daineka D, Roca i Cabarrocas P. Plasma texturing for silicon solar cells: From pyramids to inverted pyramids-like structures. *Solar Energy Materials and Solar Cells*. 2010;94(5):733-737.

14. Lin HH, Chen WH, Hong FCN. Improvement of polycrystalline silicon wafer solar cell efficiency by forming nanoscale pyramids on wafer surface using a self-mask etching technique. *Journal of Vacuum Science & Technology B*. 2013;31(3):031401.

15. Saloum S, Naddaf M, Alkhaled B. Active species characterization in RF remote oxygen plasma using actinometry OES and electrical probes. *Vacuum*. 2010;85(3):439-442.

16. Knizikevicius R. Simulations of Si and SiO2 Etching in SF6 + O2 Plasma. *Acta Physica Polonica A*. 2010;117(3):478-483.

17. Saloum S, Naddaf M, Alkhaled B. Diagnostics of N2-Ar plasma mixture excited in a 13.56 MHz hollow cathode discharge system: application to remote plasma treatment of polyamide surface. *Journal of Physics D: Applied Physics*. 2008;41(4):045205.

18. D'Agostino R, Flamm DL. Plasma etching of Si and SiO2 in SF6-O2 mixtures. *Journal of Applied Physics*. 1981;52(1):162-167.

19. Zou H. Anisotropic Si deep beam etching with profile control using SF6/O2 Plasma. *Microsystem Technologies*. 2004;10(8-9):603-607.

20. Cullis AG, Canham LT. Visible light emission due to quantum size effects in highly porous crystalline silicon. *Nature*. 1991;353:335-338.

21. Mardanian M, Nevar AA, Tarasenko NV. Optical properties of silicon nanoparticles synthesized via electrical spark discharge in water. *Applied Physics A*. 2013;112(2):437-442.

22. Qin GG, Li AP, Zhang BR, Li BC. Visible electroluminescence from semitransparent Au film/extra thin Si-rich silicon oxide film/p-Si structure. *Journal of Applied Physics*. 1995;78(3):2006-2009.

23. Zrir MA, Saloum S, Alkhaled B, Shaker SA. Revealing the role of the native oxide and the surface roughness in the visible luminescence of Ge epitaxial films. *Surface Science*. 2017;659:5-8.

24. Canham LT. Silicon quantum wire array fabrication by electrochemical and chemical dissolution of wafers. *Applied Physics Letters*. 1990;57(10):1046-1048.

25. Rittersma ZM, Splinter A, Bödecker A, Benecke W. A novel surface-micromachined capacitive porous silicon humidity sensor. *Sensors and Actuators B: Chemical*. 2000;68(1-3):210-217.